

Nonlinear Spatial Filtering in Multichannel Speech Enhancement

Kristina Tesch, *Student Member, IEEE*, and Timo Gerkmann, *Senior Member, IEEE*

Abstract—The majority of multichannel speech enhancement algorithms are two-step procedures that first apply a linear spatial filter, a so-called beamformer, and combine it with a single-channel approach for postprocessing. However, the serial concatenation of a linear spatial filter and a postfilter is not generally optimal in the minimum mean square error (MMSE) sense for noise distributions other than a Gaussian distribution. Rather, the MMSE optimal filter is a *joint spatial and spectral nonlinear* function. While estimating the parameters of such a filter with traditional methods is challenging, modern neural networks may provide an efficient way to learn the nonlinear function directly from data. To see if further research in this direction is worthwhile, in this work we examine the potential performance benefit of replacing the common two-step procedure with a joint spatial and spectral nonlinear filter.

We analyze three different forms of non-Gaussianity: First, we evaluate on super-Gaussian noise with a high kurtosis. Second, we evaluate on inhomogeneous noise fields created by five interfering sources using two microphones, and third, we evaluate on real-world recordings from the CHiME3 database. In all scenarios, considerable improvements may be obtained. Most prominently, our analyses show that a nonlinear spatial filter uses the available spatial information more effectively than a linear spatial filter as it is capable of suppressing more than $D - 1$ directional interfering sources with a D -dimensional microphone array without spatial adaptation.

Index Terms—Multichannel, speech enhancement, nonlinear spatial filtering, neural networks

I. INTRODUCTION

IN our everyday life, we are surrounded by background noise for example traffic noise or competing speakers. Hence, speech signals that are recorded in real environments are often corrupted by noise. Speech enhancement algorithms are employed to recover the target signal from a noisy recording. This is done by suppressing the background noise or reducing other unwanted effects such as reverberation. This way, speech enhancement algorithms aim to improve speech quality and intelligibility. Their fields of application are manifold and range from assisted listening devices to telecommunication all the way to automatic speech recognition (ASR) front-ends [1], [2].

If the noisy speech signal is captured by a microphone array instead of just a single microphone, then not only tempo-spectral properties can be used to extract the target signal but also spatial information. Spatial filtering aims at suppressing signal components from other than the target direction. The filter-and-sum beamforming approach [3, Sec. 12.4.2] achieves this by filtering the individual microphone signals and adding them. In the frequency domain, this means to compute the

The authors are with the Signal Processing Group, Department of Informatics, Universität Hamburg, 22527 Hamburg, Germany (e-mail: kristina.tesch@uni-hamburg.de; timo.gerkmann@uni-hamburg.de).

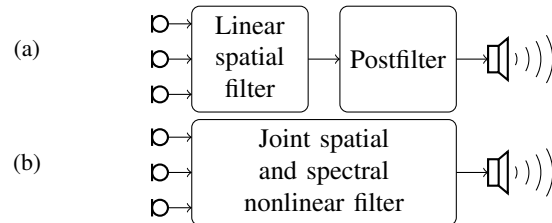


Fig. 1: (a) Illustration of the commonly employed two-step processing using a linear spatial filter (beamformer) followed by a single-channel postfilter. (b) Illustration of the nonlinear spatial filter investigated in this paper, which joins the spatial and spectral processing into a non-separable nonlinear operation.

scalar product between a complex weight vector and the vector of spectral representations of the multichannel noisy signal. Hence, the beamforming operation is linear with respect to the noisy input.

The beamforming weights are chosen to optimize some performance measure. For example, minimizing the noise variance subject to a distortionless constraint leads to the well-known minimum variance distortionless response (MVDR) beamformer [4, Sec. 3.6]. The noise suppression capability of such a spatial filter alone is often not sufficient and a single-channel filter is applied to the output of the spatial filter to improve the speech enhancement performance. The second processing stage in this two-step processing scheme is often referred to as the postfiltering step.

Single-channel speech enhancement has a long research history that has led to a variety of solutions like the classic single-channel Wiener filter [3, Sec 11.4] or other estimators derived in a statistical framework [5]–[7]. Many recent advances in single-channel speech enhancement are driven by the modeling capabilities of deep neural networks (DNNs) [8]–[11].

It seems convenient to independently develop a spatial filter and a postfilter and combine them into a two-step procedure afterward as shown in Figure 1a. If the noise follows a Gaussian distribution, this approach can even be regarded as optimal in the MMSE sense as Balan and Rosca [12] have shown that the MMSE solution can always be separated into the linear MVDR beamformer and a postfilter. However, this separability into a linear spatial filter and a postfilter only holds under the restrictive assumption that the noise is Gaussian distributed. The work of Hendriks et al. [13] points out that the MMSE optimal solution for non-Gaussian noise joins the spatial and spectral processing into a single nonlinear operation. Throughout this

work, we call such an approach a *nonlinear spatial filter* for brevity even though spectral processing steps are also included. An illustration is given in Figure 1b.

The result of Hendriks et al. reveals that the common two-step multichannel processing scheme cannot be considered optimal for more general noise distributions than a Gaussian distribution. This leads to the question if we should invest in the development of nonlinear spatial filters for example using DNNs. Today, single-channel approaches often use the possibilities of DNNs to learn complex nonlinear estimators directly from data. In contrast, the field of multichannel speech enhancement is dominated by approaches that use DNNs only for parameter estimation of a beamformer [14], [15] or restrict the network architecture in a way that a linear spatial processing model is preserved [16]. Only a few approaches with and without DNNs [17]–[19] have been proposed that extend the spatial processing model to be nonlinear. Still, the questions of how much we can possibly gain by doing this, in which situations, and also where the benefit of using a nonlinear spatial filter comes from have not been addressed adequately. These are the questions that we aim to investigate in this paper.

This work is based on a previous conference publication [20]. In [21] we have studied related aspects of these questions. Here, we extend our previous work by more detailed derivations and new analyses that provide some insight into the functioning of the nonlinear spatial filter. In Section III, we provide a detailed overview of the theoretical results from a statistical perspective. We include the previously outlined results and also provide a new simplified proof for the finding of Balan and Rosca in [12]. We then evaluate the performance benefit of a nonlinear spatial filter for heavy-tailed noise in Section IV-A, for an inhomogeneous noise field created by five interfering human speakers in Section IV-B, and real-world noise recordings in Section IV-C. In Section V, we investigate the improved exploitation of spatial information by the nonlinear spatial filter and discuss practical issues of the used analytic nonlinear spatial filter. Even though nonlinear spatial filters would most likely be implemented using DNNs in the future, in our analyses we rely on statistical MMSE estimators to provide more general insights than by using DNN-based nonlinear spatial filters which would be highly dependent on the network architecture and training data.

II. ASSUMPTIONS AND NOTATION

We assume that the signals recorded by a D -dimensional microphone array decompose into a target speech and a noise component. For each microphone-channel $\ell \in \{1, \dots, D\}$, we segment the time-domain signal into overlapping windows and transform the signal to the frequency domain using the discrete Fourier transform (DFT) to obtain the DFT coefficients $Y_\ell(k, i)$ with frequency-bin index k and time-frame index i . Throughout this work, we use segments of length 32 ms with 16 ms shift and apply the square-root Hann function for spectral analysis and synthesis. By the additive signal model, the noisy DFT coefficient can be written as the sum of the clean speech and the noise DFT coefficients $S_\ell(k, i) \in \mathbb{C}$ and $N_\ell(k, i) \in \mathbb{C}$, i.e.,

$$Y_\ell(k, i) = S_\ell(k, i) + N_\ell(k, i). \quad (1)$$

As we model the DFT coefficients to be random variables and assume independence with respect to the frequency-bin and time-frame index, we drop the indices (k, i) to simplify the notation. We indicate random variables with uppercase letters and use lowercase letters for their respective realization. Furthermore, we assume all DFT coefficients to be zero-mean and speech and noise to be uncorrelated.

We stack the noisy and noise DFT coefficients into vectors $\mathbf{Y} = [Y_1, Y_2, \dots, Y_\ell]^T \in \mathbb{C}^D$ and $\mathbf{N} = [N_1, N_2, \dots, N_\ell]^T \in \mathbb{C}^D$ and obtain the vector of speech DFT coefficients $\mathbf{S} \in \mathbb{C}^D$ by multiplying the clean speech signal coefficient $S \in \mathbb{C}$ with the so-called steering vector $\mathbf{d} \in \mathbb{C}^D$, which accounts for the propagation path between the target speaker and the microphones. We can then rewrite the signal model as

$$\mathbf{Y} = \mathbf{d}S + \mathbf{N}. \quad (2)$$

The noise correlation matrix is denoted by $\Phi_n = \mathbb{E}[\mathbf{N}\mathbf{N}^H] \in \mathbb{C}^{D \times D}$ with the statistical expectation operator \mathbb{E} and $(\cdot)^H$ denoting the Hermitian transpose. The spectral power of the target speech signal is given by $\sigma_s^2 = \mathbb{E}[|S|^2] \in \mathbb{R}^+$. When appropriate, we use the polar representation for complex-valued quantities, e.g., $s = |s|e^{j\varphi_s} \in \mathbb{C}$, and then let φ denote the phase of the complex number.

III. LINEARITY OF THE OPTIMAL SPATIAL FILTER

In this section, we aim to provide a more complete picture of the nature of the optimal spatial filter by aggregating existing results and presenting more straightforward derivations for some of these. We identify the noise distribution as the key to linearity versus non-linearity of the spatial filter and also to the separability of spatial and spectral processing. Accordingly, in our considerations we distinguish the two cases of Gaussian distributed noise and non-Gaussian distributed noise or, more precisely, noise that follows a Gaussian mixture distribution.

A. Gaussian Noise

We start with revisiting the results from Balan and Rosca [12] and then provide a simplified proof that may be easier to follow. We assume that the vector of noise DFT coefficients \mathbf{N} follows a multivariate complex Gaussian distribution with zero mean and covariance matrix Φ_n , i.e., $\mathbf{N} \sim \mathcal{CN}(0, \Phi_n)$. As we employ an additive signal model, the conditional distribution of the noisy DFT coefficient vector \mathbf{Y} given information on the reference clean speech DFT is a multivariate complex Gaussian distribution centered around the vector of clean speech DFT coefficients $\mathbf{d}s$ with the same covariance matrix Φ_n . The corresponding conditional probability density function (PDF) is given by [22, Thm. 15.1]

$$p_{\mathbf{Y}}(\mathbf{y}|s) = \frac{1}{\pi^D |\Phi_n|} \exp \left\{ -(\mathbf{y} - \mathbf{d}s)^H \Phi_n^{-1} (\mathbf{y} - \mathbf{d}s) \right\}. \quad (3)$$

Our goal is to show that the linear MVDR beamformer defined as

$$T_{\text{MVDR}}(y) = \frac{\mathbf{d}^H \Phi_n^{-1} \mathbf{y}}{\mathbf{d}^H \Phi_n^{-1} \mathbf{d}} \quad (4)$$

is the optimal spatial filter with respect to the maximum a posteriori (MAP), MMSE and maximum likelihood (ML) optimization criterion if the noise follows a Gaussian distribution.

Balan and Rosca [12] rely on the concept of sufficient statistics to prove the property in question for the MMSE optimization criterion. In our context, the MVDR beamformer T_{MVDR} is a *sufficient statistic in the Bayesian sense* if

$$p_S(s|\mathbf{y}) = p_S(s|T_{\text{MVDR}}(\mathbf{y})) \quad (5)$$

holds for every observation \mathbf{y} and every prior distribution of S [23, Thm. 2.4]. We infer from (5) that all information about S contained in the noisy observation is retained in the output of the MVDR beamformer despite the fact that the MVDR beamformer reduces the dimension of the multidimensional input to one dimension. Note that the variable of interest S in the above definition is a random variable. In contrast, T_{MVDR} is a *sufficient statistic in the classical sense* for the true clean speech DFT coefficient s , which is not assumed to be a random variable, if the conditional distribution of the noisy observation \mathbf{Y} given $T_{\text{MVDR}}(\mathbf{Y})$ does not depend on s [24, Def. IV.C.1].

As a first step, Balan and Rosca deduce that the MVDR beamformer is a sufficient statistic in the classical sense from the Fisher-Neyman factorization theorem [24, Prop. IV.C.1] [25, Cor. 2.6.1], which is applicable since the conditional PDF of the observation \mathbf{Y} given S in (3) can be rewritten as

$$\begin{aligned} p_{\mathbf{Y}}(\mathbf{y}|s) &= \frac{1}{\pi^D |\Phi_n|} \underbrace{\exp\{-\mathbf{y}^H \Phi_n^{-1} \mathbf{y}\}}_{h(\mathbf{y})} \\ &\quad \times \underbrace{\exp\left\{\mathbf{d}^H \Phi_n^{-1} \mathbf{d} (2 \operatorname{Re}\{s^* T_{\text{MVDR}}(\mathbf{y})\} - |s|^2)\right\}}_{g(s, T_{\text{MVDR}}(\mathbf{y}))} \\ &= h(\mathbf{y})g(s, T_{\text{MVDR}}(\mathbf{y})) \\ &= h(\mathbf{y})g(s, z). \end{aligned} \quad (6)$$

under the Gaussian noise assumption. In the last line of equation (6), we replaced the random variable $T_{\text{MVDR}}(\mathbf{Y})$ with Z , i.e.,

$$Z = T_{\text{MVDR}}(\mathbf{Y}), \quad (7)$$

and will now continue to use this substitute when it improves the readability. In a second step, Balan and Rosca conclude that the MVDR beamformer is a sufficient statistic in the Bayesian sense because any statistic that is sufficient in the classical sense is also sufficient in the Bayesian sense [23, Thm. 2.14.2].

We now provide a proof of the T_{MVDR} being a sufficient statistic of S in the Bayesian sense, which does not require a reference to advanced stochastic theorems. For this, we compute a factorization of the likelihood PDF of Z $p_Z(z|s)$ with Z defined in (7) as the output of the MVDR beamformer for the noisy input \mathbf{Y} . From the properties of the multivariate complex Gaussian distribution undergoing a linear transformation [22, Appx. 15B], we infer that Z given S is distributed according to a one-dimensional complex Gaussian distribution with mean s and variance $(\mathbf{d}^H \Phi_n^{-1} \mathbf{d})^{-1}$, i.e.,

$$p_Z(z|s) = \mathcal{CN}\left(s, (\mathbf{d}^H \Phi_n^{-1} \mathbf{d})^{-1}\right). \quad (8)$$

The corresponding PDF at the output of the beamformer can be factorized as

$$\begin{aligned} p_Z(z|s) &= \frac{\mathbf{d}^H \Phi_n^{-1} \mathbf{d}}{\pi} \underbrace{\exp\{-\mathbf{y}^H \Phi_n^{-1} \mathbf{y} |z|\}}_{f(\mathbf{y})} \\ &\quad \times \underbrace{\exp\left\{\mathbf{d}^H \Phi_n^{-1} \mathbf{d} (2 \operatorname{Re}\{s^* z\} - |s|^2)\right\}}_{g(s, z)} \\ &= f(\mathbf{y})g(s, z). \end{aligned} \quad (9)$$

Using (6) we rewrite the posterior distribution as

$$\begin{aligned} p_S(s|\mathbf{y}) &= \frac{p(\mathbf{y}|s)p(s)}{\int_{\mathbb{C}} p(\mathbf{y}|s)p(s)ds} \\ &= \frac{h(\mathbf{y})g(s, z)p(s)}{\int_{\mathbb{C}} h(\mathbf{y})g(s, z)p(s)ds}. \end{aligned} \quad (10)$$

Since the term $h(\mathbf{y})$ in the denominator does not depend on the integration variable s , this term cancels with the corresponding term in the numerator. Next, we extend the fraction with the term $f(\mathbf{y})$ from (9) to obtain

$$\begin{aligned} p_S(s|\mathbf{y}) &= \frac{f(\mathbf{y})g(s, z)p(s)}{\int_{\mathbb{C}} f(\mathbf{y})g(s, z)p(s)ds} \\ &= p_S(s|z) \\ &= p_S(s|T_{\text{MVDR}}(\mathbf{y})), \end{aligned} \quad (11)$$

which is the identity we wanted to prove (cf. (5)). Consequently, as the posterior given the noisy observation \mathbf{y} equals the posterior given the output of the MVDR beamformer $T_{\text{MVDR}}(\mathbf{y})$, we find that

$$T_{\text{MAP}}(\mathbf{y}) = \arg \max_{s \in \mathbb{C}} p_S(s|T_{\text{MVDR}}(\mathbf{y})) \quad (12)$$

holds. The MVDR beamformer reduces its multidimensional input to a single-channel output and, therefore, the right-hand side of (12) can be seen as a single-channel postfilter working on the output of the MVDR beamformer. Since the MMSE estimator complies with the mean of the posterior, a similar decomposition in a linear spatial filter and a spectral postfilter is given by

$$\begin{aligned} T_{\text{MMSE}}(\mathbf{y}) &= \mathbb{E}[S|\mathbf{y}] \\ &= \mathbb{E}[S|T_{\text{MVDR}}(\mathbf{y})]. \end{aligned} \quad (13)$$

Because the relationship (5) holds for all prior distributions of S , a decomposition of the MAP and MMSE estimators into a linear spatial filter followed by a postfilter exist independently from any further assumptions regarding the prior distribution of the clean speech DFT coefficient.

Finally, we consider the ML estimator. Starting from (6) and exploiting the monotony of the logarithm and Euler's formula, we find the representation

$$\begin{aligned} T_{\text{ML}}(\mathbf{y}) &= \arg \max_{s \in \mathbb{C}} p_{\mathbf{Y}}(\mathbf{y}|s) \\ &= \arg \max_{s \in \mathbb{C}} 2 \operatorname{Re}\{s^* \underbrace{T_{\text{MVDR}}(\mathbf{y})}_{=z}\} - |s|^2 \\ &= \arg \max_{s \in \mathbb{C}} 2 \cdot |s| \cdot |z| \cdot \cos(\varphi_z - \varphi_s) - |s|^2. \end{aligned} \quad (14)$$

Clearly, this function is maximized when the phase of s matches the phase of $T_{\text{MVDR}}(\mathbf{y})$, as then the cosine function is maximized. Equating the derivative with respect to $|s|$ to zero and solving for $|s|$ reveals that the magnitude of the MVDR beamformer maximizes the likelihood. Thus, $T_{\text{ML}}(\mathbf{y}) = T_{\text{MVDR}}(\mathbf{y})$, i.e. the MVDR beamformer is the maximum likelihood estimator of the clean speech DFT coefficient as also stated in [26, Sec. 6.2.1.2].

B. Non-Gaussian Noise

As we have seen, if the noise DFT coefficients follow a Gaussian distribution, then a linear spatial filter can be considered optimal. However, Hendriks et al. [13] have shown that this does not need to be the case for non-Gaussian distributed noise. In their work, they model the noise distribution with a multivariate complex Gaussian mixture distribution. The M Gaussian mixture components with respective covariance matrix Φ_m , $m \in \{1, \dots, M\}$, are assumed to be zero-mean such that the conditional PDF given the clean speech is given by

$$p_{\mathbf{Y}}(\mathbf{y}|s) = \sum_{m=1}^M c_m \mathcal{CN}(\mathbf{d}s, \Phi_m). \quad (15)$$

with mixture weights c_m that sum to one. Hendriks et al. assume that the amplitude A_S and phase φ_S of the clean speech DFT coefficient are independent. They model the phase to be uniformly distributed over the interval $[0, 2\pi)$ and assume the amplitude to be generalized-Gamma distributed ([7, Eq. 1], with $\gamma = 2$ and $\beta = \nu/\sigma_s^2$). The corresponding PDF

$$p_{A_S}(a) = 2 \frac{\left(\frac{\nu}{\sigma_s^2}\right)^\nu}{\Gamma(\nu)} a^{2\nu-1} \exp\left\{-\frac{\nu}{\sigma_s^2} a^2\right\} \quad \text{with } \nu > 0, a \geq 0 \quad (16)$$

depends on the speech shape parameter ν , and $\Gamma(\cdot)$ is the Gamma function. Under these assumptions, Hendriks et al. derive the MMSE estimator

$$T_{\text{MMSE}}(\mathbf{y}) = \nu \frac{\sum_{m=1}^M \frac{c_m Q_m}{|\Phi_m|} e^{-\mathbf{y}^H \Phi_m^{-1} \mathbf{y}} \frac{\sigma_s^2 T_{\text{MVDR}}^{(m)}(\mathbf{y}) \mathcal{M}(\nu+1, 2, P_m)}{\nu (\mathbf{d}^H \Phi_m^{-1} \mathbf{d})^{-1} + \sigma_s^2}}{\sum_{m=1}^M \frac{c_m Q_m}{|\Phi_m|} e^{-\mathbf{y}^H \Phi_m^{-1} \mathbf{y}} \mathcal{M}(\nu, 1, P_m)} \quad (17)$$

with

$$T_{\text{MVDR}}^{(m)}(\mathbf{y}) = \frac{\mathbf{d}^H \Phi_m^{-1} \mathbf{y}}{\mathbf{d}^H \Phi_m^{-1} \mathbf{d}}, \quad Q_m = (\nu + \mathbf{d}^H \Phi_m^{-1} \mathbf{d} \sigma_s^2)^{-\nu},$$

$$\text{and } P_m = \frac{\sigma_s^2 \mathbf{d}^H \Phi_m^{-1} \mathbf{d} |T_{\text{MVDR}}^{(m)}(\mathbf{y})|^2}{\nu (\mathbf{d}^H \Phi_m^{-1} \mathbf{d})^{-1} + \sigma_s^2}$$

with $\mathcal{M}(\cdot, \cdot, \cdot)$ being the confluent hypergeometric function [27, Sec. 9.21]. From (17) it is apparent that the MMSE estimator *cannot* be decomposed in a linear spatial filter and a spectral postfilter. This is because the linear term $T_{\text{MVDR}}^{(m)}$ as well as the quadratic term $\mathbf{y}^H \Phi_m^{-1} \mathbf{y}$ depend on the summation index

m . The spatial nonlinearity is particularly evident from the aforementioned quadratic term.

Throughout this work, we compare the results of the optimal spatially nonlinear MMSE estimator with a classical setup comprised of a linear spatial filter and (nonlinear) spectral postfilter. Figure 1 provides an illustration of the compared estimators: part (b) represents the nonlinear spatial filter T_{MMSE} given in (17) and part (a) corresponds to a combination of the MVDR beamformer with an MMSE-optimal postfilter. We now derive the postfilter under the same distributional assumptions as T_{MMSE} .

Since the MVDR beamformer is linear, we can infer the distribution of the beamformer output and observe that it follows a one-dimensional complex Gaussian mixture distribution with PDF

$$p(T_{\text{MVDR}}(\mathbf{y})|s) = \sum_{m=1}^M c_m \mathcal{N}_{\mathbb{C}}\left(s, \underbrace{\frac{\mathbf{d}^H \Phi_n^{-1} \Phi_m \Phi_n^{-1} \mathbf{d}}{(\mathbf{d}^H \Phi_n^{-1} \mathbf{d})^2}}_{\sigma_m^2}\right) \quad (18)$$

for an input \mathbf{Y} that is distributed according to a multivariate complex Gaussian mixture distribution. The Gaussian mixture components have the mean s and variance σ_m^2 , $m \in \{1, \dots, M\}$. Based on this observation, we compute the MMSE-optimal spectral postfilter using [27, Eq. 3.339, Eq. 6.643.2, Eq. 9.220.2] and [28, Eq. 10.32.3] and obtain the estimator

$$T_{\text{MVDR-MMSE}}(\mathbf{y}) = \frac{\sum_{m=1}^M \frac{c_m Q_m}{\sigma_m^2} e^{-\frac{|T_{\text{MVDR}}(\mathbf{y})|^2}{\sigma_m^2}} \frac{\sigma_s^2 T_{\text{MVDR}}(\mathbf{y}) \mathcal{M}(\nu+1, 2, P_m)}{\nu \sigma_m^2 + \sigma_s^2}}{\sum_{m=1}^M \frac{c_m Q_m}{\sigma_m^2} e^{-\frac{|T_{\text{MVDR}}(\mathbf{y})|^2}{\sigma_m^2}} \mathcal{M}(\nu, 1, P_m)} \quad (19)$$

with

$$\Phi_n = \sum_{m=1}^M c_m \Phi_m, \quad \sigma_m^2 = \frac{\mathbf{d}^H \Phi_n^{-1} \Phi_m \Phi_n^{-1} \mathbf{d}}{(\mathbf{d}^H \Phi_n^{-1} \mathbf{d})^2},$$

$$Q_m = \left(\frac{1}{\sigma_m^2} + \frac{\nu}{\sigma_s^2}\right)^{-\nu} \quad \text{and} \quad P_m = \frac{\sigma_s^2 \sigma_m^{-2} |T_{\text{MVDR}}(\mathbf{y})|^2}{\nu \sigma_m^2 + \sigma_s^2}.$$

that sequentially combines linear spatial processing with MMSE-optimal spectral postprocessing as depicted in Figure 1a.

IV. EVALUATION OF THE BENEFIT OF A NONLINEAR SPATIAL FILTER IN NON-GAUSSIAN NOISE

Section III points out that using a nonlinear spatial filter is MMSE-optimal and, thus, may be beneficial if the noise does not follow a Gaussian distribution. It is well known that the DFT coefficients of speech are often better modeled by a more heavy-tailed distribution than a Gaussian if originating from short-time Fourier transform (STFT) segments with short duration [6], [29]. Consequently, one may argue that this as well applies to noise DFT coefficients if the background noise stems from human speakers. In any case, Martin [29] observed that heavy-tailed distributions also provide a good fit for DFT coefficients of some types of noise in the one-dimensional case.

In this section, we investigate the potential of the optimal nonlinear spatial filter versus the classical separated setup with a linear spatial filter and a spectral postfilter for noise with a non-Gaussian distribution. Section IV-A presents our findings for noise that departs from Gaussianity by means of heavier tails but with a rather simple spatial structure. We published parts of this analysis and of the analysis in Section IV-C in [20]. However, here we also include the multichannel Wiener filter for comparison, compute more detailed performance metrics, and have made changes to the speech power parameter estimation scheme. In Section IV-B we provide results for noise that is modeling a spatially more diverse noise field created by five interfering human speakers and in Section IV-C we evaluate the nonlinear spatial filtering approach based on real-world noise recordings from the CHiME3 database. Please find audio examples for all experiments on our website¹.

A. Heavy-tailed noise distribution

In our first experiment, we investigate the performance of the nonlinear spatial filter T_{MMSE} by mixing the target speech signal at the microphones with multichannel noise that is sampled from a heavy-tailed Gaussian mixture distribution.

1) *Noise distribution model:* We construct a Gaussian mixture distribution with an adjustable heavy-tailedness by combining Gaussian components with scaled versions of the same covariance matrix. Therefore, we set the m th mixture component's covariance matrix Φ_m to be

$$\Phi_m = \frac{b^{m-1}}{r} \Phi_n \quad \text{with} \quad r = \sum_{m=1}^M c_m b^{m-1} \quad (20)$$

and scaling factor $b \in \mathbb{R}^+$. The constant r ensures correct normalization such that the overall covariance matrix of our scaled Gaussian mixture distribution remains Φ_n .

We rely on the kurtosis to quantify the heavy-tailedness of the scaled Gaussian mixture distributions. It is a statistical measure that accounts for the likelihood of the occurrence of outliers [30] and it has been extended for real-valued multivariate distributions by Mardia [31]. We extend it to complex-valued random vectors $\mathbf{X} \in \mathbb{C}^n$ with mean $\boldsymbol{\mu}$ and covariance \mathbf{C}_x by defining its kurtosis to be

$$\kappa_{\mathbb{C}}(\mathbf{X}) = \mathbb{E} \left[(2(\mathbf{X} - \boldsymbol{\mu})^H \mathbf{C}_x^{-1} (\mathbf{X} - \boldsymbol{\mu}))^2 \right]. \quad (21)$$

A complex-valued n -dimensional Gaussian distribution can equivalently be formulated as a real-valued $2n$ -dimensional Gaussian distribution [22, Thm. 15.1]. The additional factor of two in (21) ensures that the same kurtosis value results for both formulations of the same distribution. Using [32, Sec. 8.2.4], we compute the kurtosis of a vector \mathbf{N} distributed according to a scaled Gaussian mixture distribution to obtain

$$\kappa_{\mathbb{C}}(\mathbf{N}) = 2D(2 + 2D) \underbrace{\sum_{m=1}^M c_m \frac{b^{2(m-1)}}{r^2}}_q \quad (22)$$

and observe that $\kappa_{\mathbb{C}}(\mathbf{N})$ is given by the kurtosis of a D -dimensional complex Gaussian distribution multiplied by a

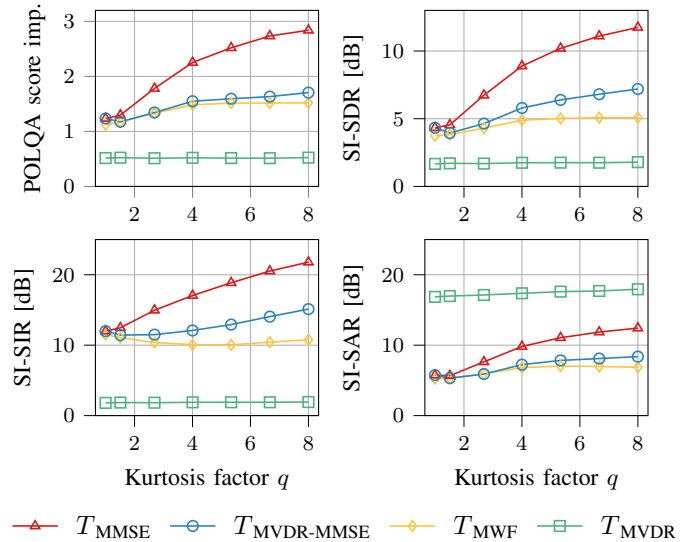


Fig. 2: perceptual objective listening quality analysis (POLQA), scale-invariant signal-to-distortion ratio (SI-SDR), scale-invariant signal-to-interference ratio (SI-SIR) and scale-invariant signal-to-artifacts ratio (SI-SAR) results for scaled Gaussian mixture noise distributions with increased heavy-tailedness in diffuse noise.

factor q that depends on the scaling factor b and the number of mixture components M .

2) *Experimental setup:* In our test scenario, we use five microphones arranged in a linear array with 5 cm spacing and broadside orientation towards the target signal source and model the propagation path between the target speaker and the microphones based on time delays only. We perform the evaluation using 48 clean speech signals taken from the WSJ0 dataset [33] that are balanced between female and male speakers. The noise DFT coefficients are samples from a scaled Gaussian mixture distribution with scale factor $b = 2$ and a variable number of mixture components with equal weight $c_m = \frac{1}{M}$, $m \in \{1, \dots, M\}$. The noise covariance matrix Φ_n models a diffuse noise field with a small portion (factor of 0.05) of additional spatially and spectrally white noise as in [34, Eq. 27]. The noise and speech are combined such that a signal-to-noise ratio (SNR) of 0 dB is obtained.

3) *Performance evaluation:* Figure 2 provides a performance comparison of the jointly spatial and spectral nonlinear T_{MMSE} and the spatially linear $T_{\text{MVDR-MMSE}}$ with a nonlinear postfilter. The speech shape parameter is set to $\nu = 0.25$ for both estimators. Furthermore, we display results obtained with the well-known linear spatial filter T_{MVDR} without a postfilter and the multichannel Wiener filter T_{MWF} , which is the MMSE-optimal solution if noise and speech follow a Gaussian distribution, i.e., $T_{\text{MVDR-MMSE}}$ with $\nu = 1$ and $M = 1$. The performance results are displayed with respect to the kurtosis factor q on the x-axis indicating an increased heavy-tailedness of the noise distribution from left to right.

The plot in the upper left corner shows the performance with respect to the improvement of the POLQA measure [35], which is the successor of perceptual evaluation of speech quality

¹<https://uhh.de/inf-sp-nonlinear-spatial-filter-tas12021>

(PESQ) [36] and returns the expected mean opinion score (MOS), which takes values from one (bad) to five (excellent). In any plot of Figure 2, we are particularly interested in the performance difference of the T_{MMSE} (red) and $T_{\text{MVDR-MMSE}}$ (blue) as this gap characterizes the potential performance gain of a nonlinear spatial filter. For POLQA, we observe an increase of the performance difference up to 1.1 POLQA score improvement as the noise distribution shifts towards a more heavy-tailed distribution.

The estimators including a postfilter, T_{MMSE} , $T_{\text{MVDR-MMSE}}$, and T_{MWF} , require an estimate of the speech power spectral density (PSD) σ_s^2 . In contrast to our previous paper [20], here we do not rely on oracle knowledge of the clean speech signal to estimate this parameter but obtain an estimate from the noisy signal based on the cepstral smoothing technique [37]. This results in an increased performance gap between T_{MMSE} and $T_{\text{MVDR-MMSE}}$. From this finding, we conclude that a nonlinear spatial filtering approach is even more beneficial if the performance of the postfilter decreases due to estimation errors of the spectral power of the target speech signal.

The next three plots (upper right and second row) display the performance results for the SI-SDR, SI-SIR, and SI-SAR measures as defined in [38]. We compute the SI-SDR, SI-SIR, and SI-SAR for segments of length 10 ms without overlap and include only segments with target speech activity similar to the computation of the segmental SNR in [39]. The performance results based on the SI-SDR measure show a similar structure to the ones obtained with POLQA. For high kurtosis values, we observe a performance gap of 4.5 dB for T_{MMSE} and $T_{\text{MVDR-MMSE}}$. Furthermore, the difference between $T_{\text{MVDR-MMSE}}$ and T_{MWF} for high kurtosis values, which results exclusively from the different postfilter, is more obvious. The observed performance gaps, in particular the performance advantage of the nonlinear spatial filter, coincide with our own listening experience¹.

For the computation of the SI-SIR and SI-SAR measure displayed in the second row, the residual noise is split into interference noise and artifacts. It is striking to see that the red graph of T_{MMSE} runs above the blue graph of $T_{\text{MVDR-MMSE}}$ in both plots meaning that the nonlinear spatial filter achieves better noise reduction and fewer speech distortions at the same time. The better performance with respect to the SI-SAR measure is quite notable as we can see that the linear MVDR beamformer introduces very few speech distortions but its combination with different postfilters ($T_{\text{MVDR-MMSE}}$ and T_{MWF}) still performs worse than the joint spatial and spectral nonlinear processing by T_{MMSE} .

B. Inhomogeneous noise field (interfering speech)

Instead of sampling a Gaussian mixture distribution as in the previous section or in [21], we now use a setup with five interfering point sources arranged as illustrated in Figure 3 and, this way, move closer towards realistic noise scenarios. The estimators T_{MMSE} and $T_{\text{MVDR-MMSE}}$ have been derived under a Gaussian mixture noise assumption. To be consistent with this modeling assumption, we require the five interfering point sources to not be Gaussian distributed or not be simultaneously

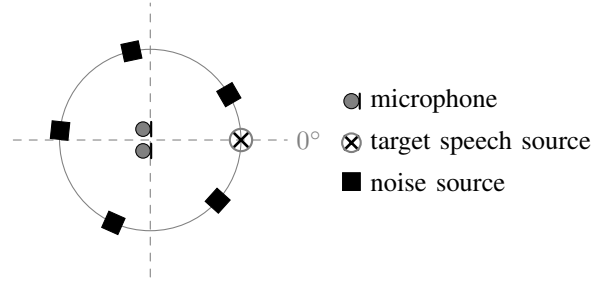


Fig. 3: Illustration of the experiment setup with a two-dimensional linear microphone array, a target speech source in broadside direction and five interfering point sources (human speakers (Section IV-B) or Gaussian bursts (Section V)).

	Interfering speech	Gaussian bursts
Δ POLQA	0.84 ± 0.04	2.64 ± 0.08
Δ SI-SDR	4.63 ± 0.15	9.92 ± 0.30
Δ SI-SAR	3.91 ± 0.16	8.39 ± 0.26
Δ SI-SIR	6.44 ± 0.22	14.95 ± 0.46
ESTOI (noisy)	0.49 ± 0.01	0.57 ± 0.02
ESTOI (T_{MMSE})	0.85 ± 0.01	0.94 ± 0.00
ESTOI ($T_{\text{MVDR-MMSE}}$)	0.72 ± 0.01	0.67 ± 0.02

TABLE I: Performance results (mean and the 95% confidence interval) of the T_{MMSE} and $T_{\text{MVDR-MMSE}}$ estimators for an inhomogeneous noise field with interfering speech and Gaussian sources as described in Section IV-B and Section V respectively.

active per time-frequency bin, because otherwise the overall noise resulting from the different interfering sources would also be Gaussian distributed. Choosing human speakers as interfering sources, this assumption is commonly assumed to hold and referred to as w-disjoint orthogonality [40].

1) *Experimental setup*: As can be seen in Figure 3, the target speech source is placed in the broadside direction of the two-dimensional linear microphone array with 6 cm microphone spacing. We sample the target speech signal and the interfering signals from distinct subsets of the WSJ0 dataset. The two-dimensional noise signal is then obtained by multiplying the interfering speech signals with the steering vectors \mathbf{d}_i , $i \in \{0, \dots, 4\}$, and adding the individual interfering sources' signals. The steering vector \mathbf{d}_i of the i th interfering source positioned at $\theta_i = \frac{\pi}{6} + \frac{2\pi}{5}i$ radians models the relative time difference of arrival at the microphones. The target speech signal and noise signal are rescaled to correspond to an SNR of 0 dB.

We now compare the performance of the T_{MMSE} and $T_{\text{MVDR-MMSE}}$ estimators for the inhomogeneous noise field. For this, we require estimates of the Gaussian mixture components' covariance matrices Φ_m and the mixture weights c_m . We choose the number of components equal to the number of interfering sources, i.e., $M = 5$, and estimate the Gaussian mixture parameters using the expectation maximization (EM) algorithm [41] applied to overlapping signal segments of length 250 ms and with an overlap of 50% from the pure noise signal. As before, we estimate the spectral power of speech using the cepstral smoothing technique and use a speech shape parameter $\nu = 0.25$.

2) *Performance evaluation*: The first column of Table I displays the performance results for the described simulation. For the performance measures in the first four rows, preceded with a Δ symbol, we report the performance difference between $T_{\text{MVDR-MMSE}}$ and T_{MMSE} averaged over 48 samples. We observe that the nonlinear spatial filter delivers a considerable performance gain that amounts to 4.63 dB SI-SDR and a POLQA score of 0.84. The bottom part of Table I presents ESTOI [42] scores for the noisy signal and the enhancement results obtained with T_{MMSE} and $T_{\text{MVDR-MMSE}}$. The ESTOI scores provide a measure of speech intelligibility. As for the other performance measures, we find that the nonlinear spatial filter outperforms the combination of a linear spatial filter and a postfilter as the T_{MMSE} estimator yields an ESTOI score of 0.85 as opposed to the result of 0.72 achieved by $T_{\text{MVDR-MMSE}}$.

C. Real-world CHiME3 noise

Furthermore, we investigate the performance of the nonlinear spatial filter for real-world noise from the CHiME3 database [43] that has been recorded in four different environments: a cafeteria, a moving bus, next to a street, and in a pedestrian area.

1) *Experimental setup*: The CHiME3 data has been recorded using six microphones that are attached to a tablet computer. For this experiment, we use the simulated training subset of the official dataset, which has been created by mixing the recording of real-world background noise with a spatialized version of WSJ0 utterances. A detailed description of the data generation process can be found in [43]. We evaluate on 48 randomly selected samples that are balanced between male and female speakers.

As before, we require an estimate of the time-varying Gaussian mixture distribution parameters and estimate them using oracle knowledge of the noise signal. For this, we apply the EM algorithm to overlapping signal segments of length 750 ms. For both, T_{MMSE} and $T_{\text{MVDR-MMSE}}$, we use $\nu = 0.25$ and estimate the speech power σ_s^2 using the cepstral smoothing technique. In addition, we need to estimate the steering vector for the target speaker. For this, we employ oracle knowledge of the clean speech signal and extract the steering vector estimates as principal eigenvectors of the time-varying covariance matrix estimates obtained by recursive smoothing.

2) *Performance evaluation*: Again, we assess the performance gap between the nonlinear spatial filter T_{MMSE} and the separated setup with a linear spatial filter and a postfilter $T_{\text{MVDR-MMSE}}$. Figure 4 displays the SI-SDR results for these estimators and also the MVDR beamformer T_{MVDR} with respect to the number of mixture components that have been fitted to a cafeteria background noise using the EM algorithm. While the performance of the T_{MMSE} estimator (red) improves with increased modeling capabilities of the mixture distribution, neither the T_{MVDR} nor the $T_{\text{MVDR-MMSE}}$ estimator benefits from using more mixture components. As a result, we observe a performance gap of 3.17 dB SI-SDR between the best result obtained with the nonlinear spatial filter and the best result obtained with the separated setup. This value coincides with the first entry of Table II. For the POLQA measure displayed in

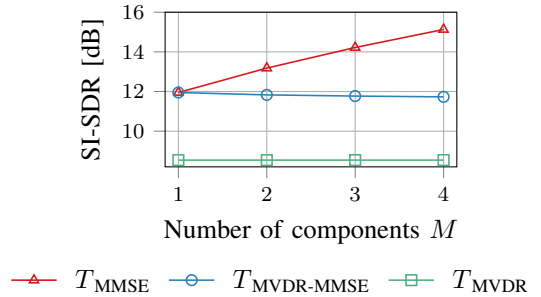


Fig. 4: SI-SDR results for cafeteria noise with respect to the number of mixture components used to fit the noise distribution.

	CAF	BUS	PED	STR
Δ SI-SDR	3.17 \pm 0.19	2.48 \pm 0.26	3.31 \pm 0.24	2.07 \pm 0.28
Δ POLQA	0.59 \pm 0.06	0.38 \pm 0.07	0.56 \pm 0.05	0.28 \pm 0.04
ESTOI (noisy)	0.60 \pm 0.03	0.71 \pm 0.02	0.56 \pm 0.03	0.69 \pm 0.03
ESTOI (T_{MMSE})	0.94 \pm 0.01	0.97 \pm 0.01	0.93 \pm 0.01	0.96 \pm 0.01
ESTOI ($T_{\text{MVDR-MMSE}}$)	0.89 \pm 0.02	0.95 \pm 0.01	0.88 \pm 0.02	0.94 \pm 0.01

TABLE II: Performance results (mean and the 95% confidence interval) of the nonlinear spatial T_{MMSE} and linear spatial filter combined with a postfilter $T_{\text{MVDR-MMSE}}$ for noise from the CHiME3 database, which has been fitted with a Gaussian mixture distribution with four mixture components as described in Section IV-C.

the second row, we find a difference of 0.59 POLQA score. The table shows bigger performance differences for the cafeteria (CAF) and pedestrian area (PED) noise than the bus (BUS) and street (STR) noise. We suppose that this reflects that the cafeteria and pedestrian area noise is less stationary as we hear the most significant differences for impulse like background noise. The ESTOI scores displayed at the bottom of Table II indicate that the nonlinear spatial filter is not only beneficial to the speech quality but also the speech intelligibility. Overall, we conclude that the Gaussian noise assumption does not seem to be valid for the examined real-world noise as the nonlinear spatial filter provides a notable benefit also for these recordings.

V. INTERPRETATION: A NONLINEAR SPATIAL FILTER ENABLES SUPERIOR SPATIAL SELECTIVITY

We assume that the performance benefit of the nonlinear spatial filter reported in Section IV-B and IV-C is due to the more efficient use of spatial information by the T_{MMSE} estimator. Here we support this conjecture by an experiment that provides an insight into the functioning of the nonlinear spatial filter.

1) *Experimental setup*: We use the same geometric setup as described previously in Section IV-B (Figure 3) but replace the interfering speech sources with sources that emit spectrally white Gaussian signals. To match the long-term non-Gaussianity assumption, only one interfering source emits a signal at a specific time instance. We implement this by using short (336 ms) non-overlapping Gaussian bursts for the interfering sources. The so created noise signal can be viewed as stationary

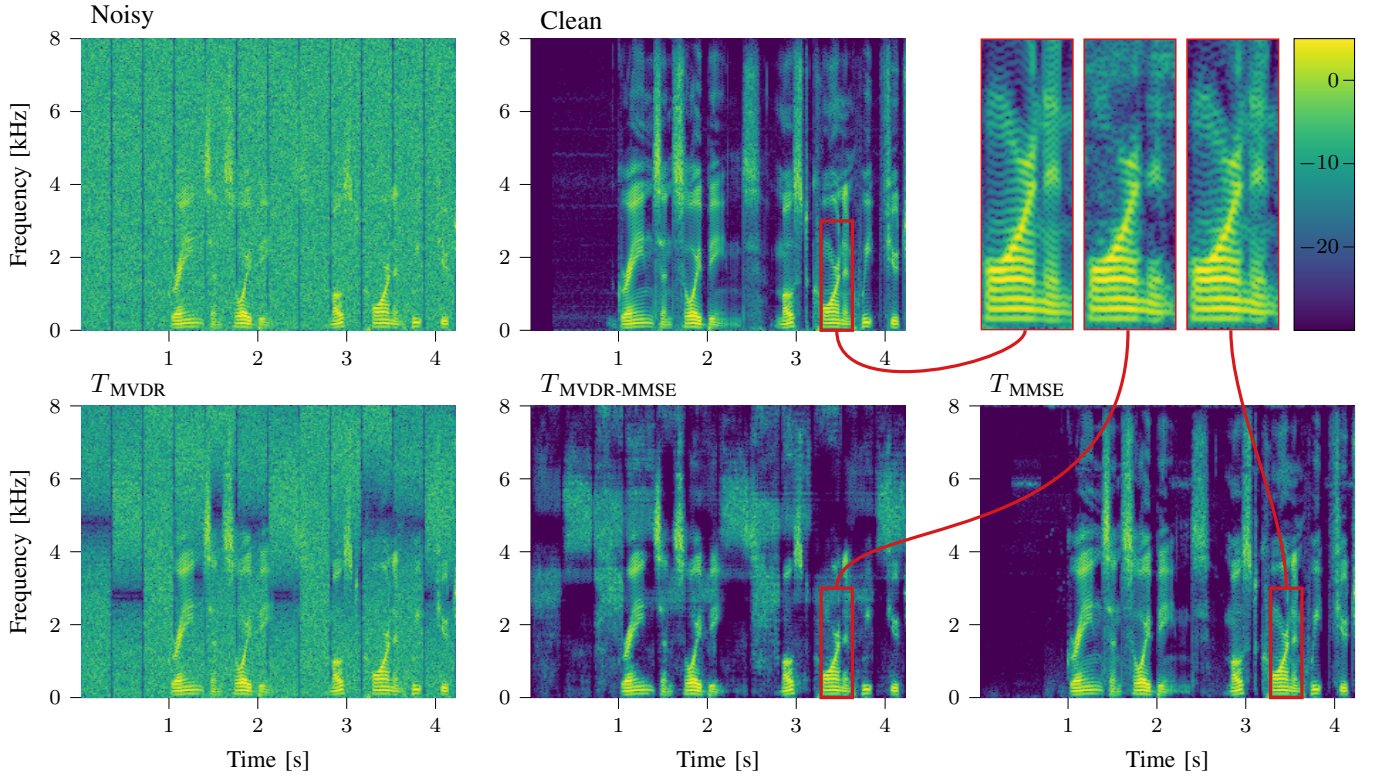


Fig. 5: Spectrograms of an example in an inhomogeneous noise field with five interfering sources emitting Gaussian noise bursts. The second row visualizes the processing results obtained with T_{MVDR} , $T_{MVDR-MMSE}$ and T_{MMSE} and the top row shows the clean and noisy spectrograms as well as close-ups of the fine-structure of a voiced speech segment.

regarding its spectral characteristics except at the segment boundaries. By applying the EM algorithm to the full-length noise signal we also model the spatial characteristics as long-term stationary. All other experiment settings remain unchanged as described before in Section IV-B.

2) *Performance evaluation*: The performance results are displayed in the second column of Table I. For this artificial type of noise, we observe an even greater performance difference of 9.9 dB SI-SDR and 2.6 POLQA score. In fact, the T_{MMSE} estimator seems to be able to recover the original signal almost perfectly except from minor residual high-frequency noise while $T_{MVDR-MMSE}$ suffers from clearly audible speech degradation and residual noise. Audio examples can be found online¹.

Figure 5 depicts the spectrograms of the clean and noisy signals in the top row and the spectrograms of the enhancement results obtained by the T_{MVDR} , $T_{MVDR-MMSE}$, and T_{MMSE} estimators in the bottom row. The uniform green coloration of the vertical stripes in the noisy spectrogram reflects the spectral stationarity. The vertical dark blue lines separate segments with different spatial properties. While the spatial diversity cannot be seen from the spectrogram, it becomes visible from the result of the MVDR beamformer (first in bottom row). Here, the MVDR beamformer suppresses different frequencies for signal segments with different spatial properties as can be seen from the displaced horizontal dark blue lines. The described differences between the $T_{MVDR-MMSE}$ (middle) and T_{MMSE}

(right) estimators' results are also found in the spectrograms. A close look reveals that the nonlinear spatial filter preserves much more of the target signal's fine structure. Furthermore, a comparison with the spectrogram of the clean speech signal highlights that it suppresses background noise much better than the $T_{MVDR-MMSE}$ estimator. Residual noise is visible in the spectrogram only in some segments at a frequency of about 6 kHz.

3) *Discussion*: To explain these observations, we examine the covariance matrices Φ_m , $m \in \{1, \dots, 5\}$, of the Gaussian mixture noise distribution estimated with the EM algorithm. In Figure 6 we visualize their spatial structure based on the directivity pattern [3, Sec. 12.5.2] that they produce when used as noise correlation matrix in the MVDR beamformer, which is denoted with $T_{MVDR}^{(m)}$ in (17). Furthermore, we visualize the directivity pattern of the MVDR beamformer. The correlation matrix Φ_n required to compute T_{MVDR} is related to the mixture component covariance matrices via

$$\Phi_n = \sum_{m=1}^M c_m \Phi_m. \quad (23)$$

The directivity pattern produced by T_{MVDR} is displayed at the top left followed by visualizations of the five mixture component covariance matrices. For each of these, a pronounced spatial characteristic can be observed by means of the horizontal dark lines. On the right side of the directivity patterns, we indicate the incidence angles θ_i of the noise sources. We notice

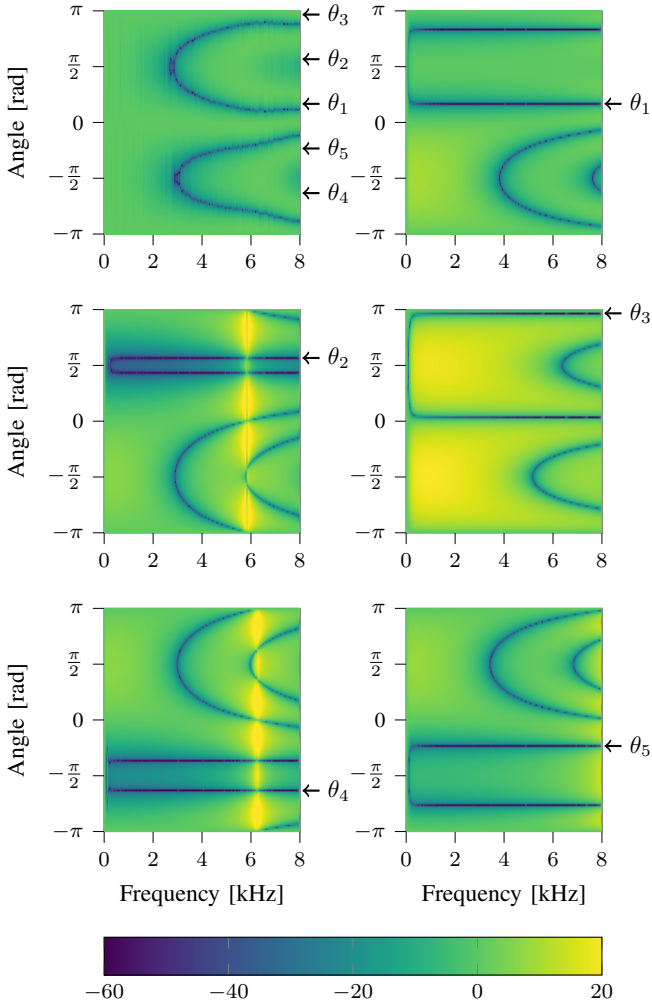


Fig. 6: Directivity patterns of T_{MVDR} (top left) and $T_{\text{MVDR}}^{(m)}$ (MVDR beamformer with noise correlation matrix Φ_m), $m \in \{1, \dots, 5\}$. The arrows on the right side indicate the incidence angle θ_i , $i \in \{0, \dots, 4\}$ of the i th interfering point source.

that each component’s covariance matrix models one of the noise sources as apparent from the zero placed in the respective direction by the MVDR beamformer. The second horizontal line originates from the symmetry requirements of the directivity pattern, which are determined by the array geometry.

In comparison, the directivity pattern of the T_{MVDR} (top left) does not show zeros placed into the directions of the interfering point sources. Instead, the weighted combination in (23) seems to eliminate some of the spatial information, which corresponds to the well-known fact that a two-microphone MVDR beamformer can suppress only one directional interfering source but not five of them. As a result, only some frequencies are suppressed for each interfering source as we observed in Figure 5 before.

Figure 6 reveals how much more spatial information can be utilized by T_{MMSE} in comparison with $T_{\text{MVDR-MMSE}}$, whose spatial processing relies on an estimate of Φ_n as visualized in the top left plot. The initial spatial filtering step using the MVDR beamformer is not capable of suppressing the

directional sources and the remaining noise has to be filtered by the postfilter, which then leads to some improvements. On the other hand, the nonlinear spatial T_{MMSE} estimator can utilize the spatial information provided by the estimates of covariance matrices Φ_m .

One could argue that a time-varying MVDR beamformer $T_{\text{MVDR}}^{(m)}$ with correctly chosen m would suffice to solve the problem on the short signal segments with noise from a single point source and a complicated nonlinear approach is not required. However, we must point out that the step of choosing the ‘right’ covariance matrix is not required for the nonlinear spatial filter. Instead, we provide the Gaussian mixture parameters reflecting the spatial properties of the full utterance and, nevertheless, the T_{MMSE} estimator is capable of suppressing five directional noise sources with only two microphones without the need for spatial adaptation. Note that this is an exciting finding as traditional linear spatial filters can only suppress $D - 1$ interfering point sources with D microphones without spatial adaptation [26, Sec. 6.3].

Despite the impressive performance results achieved in this experiment, the analytic nonlinear spatial filter has some weaknesses: it requires a very accurate estimation of the spatial and spectral characteristics of the noise signal and is also computationally quite demanding. In addition to the presented experiments, we carried out simulations using measured impulse responses between the microphones and speakers and observed a much lower benefit from using a nonlinear spatial filter for the experiment with five interfering Gaussian sources even with access to oracle noise data. This is because the spatial and spectral diversity of the noise signal increase and many more mixture components would be required to model the noise accurately which then results in a data problem. Similarly, estimating the parameters of the Gaussian mixture from a noisy signal is difficult. We approached this using masks to identify time-frequency bins that are dominated by noise but did not obtain reliable estimates this way.

Therefore, we conclude that the analytical estimators allow us to study the potential of nonlinear spatial filters in principle, but because of high sensitivity to parameter estimation errors and high computational costs, practical nonlinear spatial filters may be better implemented using modern machine learning tools like DNNs.

VI. CONCLUSIONS

In a detailed theory overview, we have revisited the fact that the multichannel MMSE-optimal estimator of the clean speech signal is in general a jointly spatial-spectral nonlinear filter. Therefore, the state-of-the-art concatenation of a linear spatial filter and a postfilter is MMSE-optimal only in the special case that the noise follows a Gaussian distribution. The experimental section of this paper studied the performance advantage that can be gained by replacing the generally suboptimal sequential setup with a nonlinear spatial filter in three different non-Gaussian noise scenarios.

First, we have shown that considerable performance improvements result if the noise distribution deviates from a Gaussian distribution by an increased heavy-tailedness as the

nonlinear spatial filter enables a higher noise reduction and lower speech distortions at the same time. Second, we report a performance benefit of 4.6 dB SI-SDR and of 0.8 POLQA score for an inhomogeneous noise field created by five interfering speech sources and, furthermore, we have observed a benefit of about 3.2 dB SI-SDR and 0.6 POLQA score for the real-world cafeteria noise recordings from the CHiME3 database. In addition, we have performed experiments that revealed that the nonlinear spatial filter has some notably increased spatial processing capabilities allowing for an almost perfect elimination of five Gaussian interfering point sources with only two microphones.

The presented findings on the performance potential of a nonlinear spatial filter motivate further research on the implementation of nonlinear spatial filters, e.g., using DNNs to learn the nonlinear spatial filter directly from data and overcome the parameter estimation issues and other limitations of the analytic nonlinear spatial filter that we have used for this analysis.

ACKNOWLEDGMENT

We would like to thank J. Berger and Rohde&Schwarz SwissQual AG for their support with POLQA.

REFERENCES

- [1] S. Doclo, W. Kellermann, S. Makino, and S. E. Nordholm, "Multichannel Signal Enhancement Algorithms for Assisted Listening Devices: Exploiting spatial diversity using multiple microphones," *IEEE Signal Processing Magazine*, vol. 32, no. 2, pp. 18–30, Mar. 2015.
- [2] F. Weninger, H. Erdogan, S. Watanabe, E. Vincent, J. Le Roux, J. R. Hershey, and B. Schuller, "Speech enhancement with LSTM recurrent neural networks and its application to noise-robust ASR," in *International Conference on Latent Variable Analysis and Signal Separation (LVA/ICA)*, Liberec, Czech Republic, Aug. 2015.
- [3] P. Vary and R. Martin, *Digital speech transmission: enhancement, coding and error concealment*. Chichester, England Hoboken, NJ: John Wiley, 2006.
- [4] J. Benesty, *Microphone Array Signal Processing*. Berlin: Springer, 2008.
- [5] Y. Ephraim and D. Malah, "Speech enhancement using a minimum-mean square error short-time spectral amplitude estimator," *IEEE Transactions on Acoustics, Speech, and Signal Processing*, vol. 32, no. 6, pp. 1109–1121, Dec. 1984.
- [6] T. Lotter and P. Vary, "Speech Enhancement by MAP Spectral Amplitude Estimation Using a Super-Gaussian Speech Model," *EURASIP Journal on Advances in Signal Processing*, vol. 2005, no. 7, pp. 1110–1126, May 2005.
- [7] J. S. Erkelens, R. C. Hendriks, R. Heusdens, and J. Jensen, "Minimum Mean-Square Error Estimation of Discrete Fourier Coefficients With Generalized Gamma Priors," *IEEE Transactions on Audio, Speech, and Language Processing*, vol. 15, pp. 1741–1752, 2007.
- [8] Y. Xu, J. Du, L. Dai, and C. Lee, "A regression approach to speech enhancement based on deep neural networks," *IEEE/ACM Transactions on Audio, Speech, and Language Processing*, vol. 23, no. 1, pp. 7–19, Jan. 2015.
- [9] D. Rethage, J. Pons, and X. Serra, "A Wavenet for Speech Denoising," in *2018 IEEE International Conference on Acoustics, Speech and Signal Processing (ICASSP)*, Apr. 2018, pp. 5069–5073.
- [10] S. R. Park and J. Lee, "A Fully Convolutional Neural Network for Speech Enhancement," in *Proc. Interspeech 2017*, Stockholm, Sweden, 2017, pp. 1993–1997.
- [11] A. Pandey and D. Wang, "TCNN: Temporal Convolutional Neural Network for Real-time Speech Enhancement in the Time Domain," in *2019 IEEE International Conference on Acoustics, Speech and Signal Processing (ICASSP)*, Brighton, United Kingdom, 2019, pp. 6875–6879.
- [12] R. Balan and J. P. Rosca, "Microphone Array Speech Enhancement by Bayesian Estimation of Spectral Amplitude and Phase," in *Sensor Array and Multichannel Signal Processing Workshop Proceedings*, Rosslyn, Virginia, Aug. 2002, pp. 209–213.
- [13] R. C. Hendriks, R. Heusdens, U. Kjems, and J. Jensen, "On Optimal Multichannel Mean-Squared Error Estimators for Speech Enhancement," *IEEE Signal Processing Letters*, vol. 16, pp. 885–888, 2009.
- [14] J. Heymann, L. Drude, and R. Haeb-Umbach, "Neural network based spectral mask estimation for acoustic beamforming," in *2016 IEEE International Conference on Acoustics, Speech and Signal Processing (ICASSP)*, Shanghai, China, Mar. 2016, pp. 196–200.
- [15] X. Xiao, S. Watanabe, H. Erdogan, L. Lu, J. Hershey, M. L. Seltzer, G. Chen, Y. Zhang, M. Mandel, and D. Yu, "Deep beamforming networks for multi-channel speech recognition," in *2016 IEEE International Conference on Acoustics, Speech and Signal Processing (ICASSP)*, Shanghai, China, 2016, pp. 5745–5749.
- [16] T. N. Sainath, R. J. Weiss, K. W. Wilson, B. Li, A. Narayanan, E. Variiani, M. Bacchiani, I. Shafran, A. Senior, K. Chin, A. Misra, and C. Kim, "Multichannel signal processing with deep neural networks for automatic speech recognition," *IEEE/ACM Transactions on Audio, Speech, and Language Processing*, vol. 25, no. 5, pp. 965–979, May 2017.
- [17] H. Lee, H. Y. Kim, W. H. Kang, J. Kim, and N. S. Kim, "End-to-End Multi-Channel Speech Enhancement Using Inter-Channel Time-Restricted Attention on Raw Waveform," in *Proc. Interspeech 2019*. Graz, Austria: ISCA, Sep. 2019, pp. 4285–4289.
- [18] B. Tolooshams, R. Giri, A. H. Song, U. Isik, and A. Krishnaswamy, "Channel-Attention Dense U-Net for Multichannel Speech Enhancement," in *2020 IEEE International Conference on Acoustics, Speech and Signal Processing (ICASSP)*, Barcelona, Spain, May 2020, pp. 836–840.
- [19] G. Itzhak, J. Benesty, and I. Cohen, "Nonlinear Kronecker product filtering for multichannel noise reduction," *Speech Communication*, vol. 114, pp. 49–59, Nov. 2019.
- [20] K. Tesch, R. Rehr, and T. Gerkmann, "On Nonlinear Spatial Filtering in Multichannel Speech Enhancement," in *Proc. Interspeech 2019*, Graz, Austria, 2019, pp. 91–95.
- [21] K. Tesch and T. Gerkmann, "Nonlinear spatial filtering for multichannel speech enhancement in inhomogeneous noise fields," in *2020 IEEE International Conference on Acoustics, Speech and Signal Processing*, Barcelona, Spain, May 2020, pp. 196–200.
- [22] S. M. Kay, *Fundamentals Of Statistical Signal Processing*. Pearson, 2009.
- [23] M. Schervish, *Theory of Statistics*. New York, NY: Springer New York, 1995.
- [24] H. Poor, *An Introduction to Signal Detection and Estimation*. New York, NY: Springer New York, 1994.
- [25] E. L. Lehmann, *Testing Statistical Hypotheses*. New York: Springer, 2005.
- [26] H. L. V. Trees, *Optimum Array Processing: Part IV of Detection, Estimation, and Modulation Theory*. John Wiley & Sons, Apr. 2004.
- [27] I. S. Gradshteyn and J. M. Ryzhik, *Table of Integrals, Series, and Products*. San Diego: Academic Press, 2000.
- [28] "NIST Digital Library of Mathematical Functions," f. W. J. Olver, A. B. Olde Daalhuis, D. W. Lozier, B. I. Schneider, R. F. Boisvert, C. W. Clark, B. R. Miller and B. V. Saunders, eds.
- [29] R. Martin, "Speech enhancement based on minimum mean-square error estimation and supergaussian priors," *IEEE Transactions on Speech and Audio Processing*, vol. 13, no. 5, pp. 845–856, Sep. 2005.
- [30] P. H. Westfall, "Kurtosis as Peakedness, 1905–2014. R.I.P.," *The American Statistician*, vol. 68, no. 3, pp. 191–195, 2014.
- [31] K. V. Mardia, "Measures of Multivariate Skewness and Kurtosis with Applications," *Biometrika*, vol. 57, no. 3, pp. 519–530, 1970.
- [32] K. B. Petersen and M. S. Pedersen, "The Matrix Cookbook," Nov. 2012.
- [33] J. S. Garofolo, D. Graff, D. Paul, and D. Pallett, "CSR-I (WSJ0) Complete LDC93S6A," Linguistic Data Consortium, Philadelphia, May 2007.
- [34] C. Pan, J. Chen, and J. Benesty, "Performance study of the MVDR beamformer as a function of the source incidence angle," *IEEE/ACM Transactions on Audio, Speech, and Language Processing*, vol. 22, no. 1, pp. 67–79, Jan. 2014.
- [35] "P.863: Perceptual objective listening quality prediction," International Telecommunication Union, Mar. 2018, iTU-T recommendation. [Online]. Available: <https://www.itu.int/rec/T-REC-P.863-201803-I/en>
- [36] "P.862.3: Application guide for objective quality measurement based on Recommendations P.862, P.862.1 and P.862.2," International Telecommunication Union, Nov. 2007, iTU-T recommendation. [Online]. Available: <https://www.itu.int/rec/T-REC-P.862.3-200711-I/en>
- [37] C. Breithaupt, T. Gerkmann, and R. Martin, "A novel a priori SNR estimation approach based on selective cepstro-temporal smoothing," in *2008 IEEE International Conference on Acoustics, Speech and Signal Processing (ICASSP)*, Las Vegas, USA, Mar. 2008, pp. 4897–4900.

- [38] J. L. Roux, S. Wisdom, H. Erdogan, and J. R. Hershey, “SDR – Half-baked or Well Done?” in *2019 IEEE International Conference on Acoustics, Speech and Signal Processing (ICASSP)*, Brighton, United Kingdom, May 2019, pp. 626–630.
- [39] T. Gerkmann and R. C. Hendriks, “Unbiased MMSE-Based Noise Power Estimation With Low Complexity and Low Tracking Delay,” *IEEE Transactions on Audio, Speech, and Language Processing*, vol. 20, no. 4, pp. 1383–1393, May 2012.
- [40] O. Yilmaz and S. Rickard, “Blind separation of speech mixtures via time-frequency masking,” *IEEE Transactions on Signal Processing*, vol. 52, no. 7, pp. 1830–1847, Jul. 2004.
- [41] C. Bishop, *Pattern recognition and machine learning*. New York: Springer, 2006.
- [42] J. Jensen and C. H. Taal, “An algorithm for predicting the intelligibility of speech masked by modulated noise maskers,” *IEEE/ACM Transactions on Audio, Speech, and Language Processing*, vol. 24, no. 11, pp. 2009–2022, 2016.
- [43] J. Barker, R. Marxer, E. Vincent, and S. Watanabe, “The third ‘CHiME’ speech separation and recognition challenge: Dataset, task and baselines,” in *IEEE Workshop on Automatic Speech Recognition and Understanding (ASRU)*, Scottsdale, USA, Dec. 2015, pp. 504–511.



Kristina Tesch (S’20) received a B.Sc and M.Sc in Informatics in 2016 and 2019 from the Universität Hamburg, Hamburg, Germany. She is with the Signal Processing Group at the Universität Hamburg since 2019 and is currently working towards a doctoral degree. Her research interests include digital signal processing and machine learning algorithms for speech and audio with a focus on multichannel speech enhancement. For her master thesis on multichannel speech enhancement, she received the award for the best master thesis at a German Informatics

Department from the Fakultätentag Informatik in 2019.



Timo Gerkmann (S’08–M’10–SM’15) studied Electrical Engineering and Information Sciences at the Universität Bremen and the Ruhr-Universität Bochum in Germany. He received his Dipl.-Ing. degree in 2004 and his Dr.-Ing. degree in 2010 both in Electrical Engineering and Information Sciences from the Ruhr-Universität Bochum, Bochum, Germany. In 2005, he spent six months with Siemens Corporate Research in Princeton, NJ, USA. During 2010 to 2011 Dr. Gerkmann was a postdoctoral researcher at the Sound and Image Processing Lab at the Royal Institute of

Technology (KTH), Stockholm, Sweden. From 2011 to 2015 he was a professor for Speech Signal Processing at the Universität Oldenburg, Oldenburg, Germany. During 2015 to 2016 he was a Principal Scientist for Audio & Acoustics at Technicolor Research & Innovation in Hanover, Germany. Since 2016 he is a professor for Signal Processing at the Universität Hamburg, Germany. His main research interests are on statistical signal processing and machine learning for speech and audio applied to communication devices, hearing instruments, audio-visual media, and human-machine interfaces. Timo Gerkmann serves as an elected member of the IEEE Signal Processing Society Technical Committee on Audio and Acoustic Signal Processing and as an Associate Editor of the IEEE/ACM Transactions on Audio, Speech and Language Processing.